PNAS RESEARCH ARTICLE | CELL BIOLOGY

Targeting ON-bipolar cells by AAV gene therapy stably reverses *LRIT3*-congenital stationary night blindness

Keiko Miyadera[a,1], Evelyn Santana[a], Karolina Roszak[a], Sommer Iffrig[a], Meike Visel[b], Simone Iwabe[c], Ryan F. Boyd[c], Joshua T. Bartoe[c], Yu Sato[a], Alexa Gray[a], Ana Ripolles-Garcia[a], Valérie L. Dufour[a], Leah C. Byrne[b,d], John G. Flannery[b], William A. Beltran[a], and Gustavo D. Aguirre[a]

Edited by Alessandro Iannaccone, Duke University, Durham, NC; received October 12, 2021; accepted January 10, 2022 by Editorial Board Member Jeremy Nathans

Adeno-associated virus (AAV)–based gene therapies aimed at curing inherited retinal diseases to date have typically focused on photoreceptors and retinal pigmented epithelia within the relatively accessible outer retina. However, therapeutic targeting in diseases such as congenital stationary night blindness (CSNB) that involve defects in ON-bipolar cells (ON-BCs) within the midretina has been challenged by the relative inaccessibility of the target cell in intact retinas, the limited transduction efficiency of these cells by existing AAV serotypes, poor availability of established ON-BC–specific promoters, and the absence of appropriate patient-relevant large animal models. Here, we demonstrate safe and effective ON-BC targeting by AAV gene therapy in a recently characterized naturally occurring canine model of CSNB: leucine-rich repeat, immunoglobulin-like and transmembrane domain 3 (*LRIT3*)–CSNB. To effectively target ON-BCs, AAV capsid variants with ON-BC tropism and ON-BC–specific modified GRM6 promoters were adopted to ensure cell-specific transgene expression. Subretinal injection of one vector, AAV$^{K9\#4}$-*sh*GRM6-c*LRIT3*-WPRE, significantly recovered rod-derived b-wave in all treated eyes (six of six) of adult dogs injected at 1 to 3 y of age. The robust therapeutic effect was evident 7 wk postinjection and sustained for at least 1 y in all treated eyes. Scotopic vision was significantly improved in treated eyes based on visually guided obstacle course navigation. Restoration of LRIT3 signals was confirmed by immunohistochemistry. Thus, we report ON-BC functional rescue in a large animal model using an AAV capsid variant and modified promoter construct optimized for ON-BC specificity, thereby establishing both proof of concept and a translational platform for treatment of CSNB in patients with defects in photoreceptor-to-bipolar signaling.

congenital stationary night blindness | animal model | ON-bipolar cells | LRIT3 | AAV

Significance

Canine models of inherited retinal diseases have helped advance adeno-associated virus (AAV)–based gene therapies targeting specific cells in the outer retina for treating blinding diseases in patients. However, therapeutic targeting of diseases such as congenital stationary night blindness (CSNB) that exhibit defects in ON-bipolar cells (ON-BCs) of the midretina remains underdeveloped. Using a leucine-rich repeat, immunoglobulin-like and transmembrane domain 3 (*LRIT3*) mutant canine model of CSNB exhibiting ON-BC dysfunction, we tested the ability of cell-specific AAV capsids and promotors to specifically target ON-BCs for gene delivery. Subretinal injection of one vector demonstrated safety and efficacy with robust and stable rescue of electroretinography signals and night vision up to 1 y, paving the way for clinical trials in patients.

The vision process begins with photon capture by outer segments of rods and cones, photoreceptors within the outer retina. Subsequent release of neurotransmitters by photoreceptor synaptic terminals—rod spherules and cone pedicles—transfers this information to bipolar cell dendritic processes in the outer plexiform layer (OPL). Notably, distinct cell classes and signaling pathways allow for day and night vision. Specifically, night vision requires signaling from rod photoreceptors to ON-bipolar cells (ON-BCs) and activation of the metabotropic glutamate receptor 6 (mGluR6) signaling cascade at the dendritic tips of ON-BCs. In the dark, glutamate is released from photoreceptor terminals, binds to mGluR6, and activates the α-subunit of a G protein, Goα. Dissociation of G-protein subunits culminates in the closure of transient receptor potential melastatin 1 (TRPM1) channels, the key regulator of the mGluR6 signaling cascade (1). Several molecules, including leucine-rich repeat, immunoglobulin-like and transmembrane domain 3 (LRIT3) and nyctalopin (NYX), are critical in localizing TRPM1 to the ON-BC dendritic tip membrane (2). Inherited defects in this pathway, from photon capture, phototransduction, neurotransmitter release, and mGluR6 signaling, cause nonprogressive vision-impairing disorders, termed congenital stationary night blindness (CSNB), that are characterized by the absence of night vision from birth.

The genetically heterogeneous causation of CSNB (3) underlies the spectrum of clinical presentations, broadly classified using electroretinography (ERG) as Riggs (4) and Schubert–Bornschein (5) forms of CSNBs. The Riggs type is caused by defects in photoreceptors and is associated to date with four genes, *RHO*, *GNAT1*, *PDE6B*, and *SLC24A1*, in decreasing order of prevalence (3). The Schubert–Bornschein type results from erroneous photoreceptor-to-bipolar cell signaling and is further subdivided into incomplete CSNB and complete congenital stationary night blindness (cCSNB) (6). Incomplete CSNB is associated with partial blockage of photoreceptor-to-bipolar cell signaling that results in some residual rod function. Defects in three genes, *CACNA1F*,

Author contributions: K.M., L.C.B., W.A.B., and G.D.A. designed research; K.M., E.S., K.R., S. Iffrig, M.V., S. Iwabe, Y.S., A.G., A.R.-G., and V.L.D. performed research; M.V., R.F.B., J.T.B., L.C.B., J.G.F., and W.A.B. contributed new reagents/analytic tools; K.M., E.S., K.R., S. Iffrig, Y.S., A.G., A.R.-G., V.L.D., L.C.B., W.A.B., and G.D.A. analyzed data; and K.M., W.A.B., and G.D.A. wrote the paper.

The authors declare no competing interest.

This article is a PNAS Direct Submission. A.I. is a guest editor invited by the Editorial Board.

[1]To whom correspondence may be addressed. Email: kmiya@upenn.edu.

This article contains supporting information online at http://www.pnas.org/lookup/suppl/doi:10.1073/pnas.2117038119/-/DCSupplemental.

Published March 22, 2022.

CABP4, and *CACNA2D4*, all expressed presynaptically in the photoreceptor terminals are associated with incomplete CSNB (3). cCSNB is the most common form, and patients exhibit characteristic ERG features, including extinguished scotopic b-wave due to ON-BC dysfunction. Defects in five genes, *NYX* (7, 8), *TRPM1* (9–11), *GRM6* (12, 13), *GPR179* (14, 15), and *LRIT3* (16), all historically thought to localize postsynaptically in the ON-BC dendritic tips are associated with cCSNB.

A series of cCSNB mouse models with ON-BC defects is categorized as "*nob*" (no b-wave) mice (3). Consistent with the nonprogressive nature of CSNB, *Lrit3*-deficient mice ($Lrit3^{-/-}$, $Lrit3^{nob6}$) have an intact outer nuclear layer (17), and the observed cone-specific disorganization of synaptic contacts supports a role for LRIT3 in transsynaptic communication between cones and ON-BCs (18). As with other *nob* mouse models, *Lrit3*-deficient *nob6* mice only partially recapitulate the phenotype of *LRIT3*-cCSNB human patients due to unexpected loss of photopic b-waves in addition to expected loss of scotopic b-waves (*SI Appendix*, Table S1) (16, 17).

We have previously characterized a naturally occurring canine model of CSNB with striking night blindness and normal day vision. Full-field ERGs showed a predominant loss of scotopic b-waves, consistent with Schubert–Bornschein-type cCSNB (19). A subsequent genome-wide association study and whole-genome sequencing identified an exonic 1-base pair (bp) insertion in *LRIT3* (20), a gene associated with cCSNB in both patients (16) and the murine model (17). Canine leucine-rich repeat, immunoglobulin-like and transmembrane domain 3 (cLRIT3) is predicted to have a signal peptide; two LRRs (leucine-rich repeats); two LRR-type domains; and one each of LRR C-terminal, IGc2, fibronectin type III (FN3), and transmembrane domains. The c*LRIT3* disease variant generated a premature stop codon, giving rise to a truncated LRIT3 predicted to lack IGc2, FN3, and C-terminal transmembrane domains (20). *In vitro* studies showed that subcellular expression and distribution of the truncated LRIT3 were comparable with wild-type (WT) LRIT3, indicating that this nonfunctional variant does not necessarily negatively affect cell survival. Moreover, immunohistochemistry (IHC) analysis showed punctate LRIT3 labeling in putative ON-BC dendritic terminals colabeled with Goα in WT but markedly decreased levels in the mutants (20), suggesting that *LRIT3* augmentation might be an effective approach for therapeutic intervention. To target ON-BCs more effectively in mature retina, we screened a small pool of adeno-associated virus (AAV) capsid variants for ON-BC tropism in adult dogs. Herein, we report ON-BC functional rescue in a large animal model using an AAV variant and a modified promoter, both designed for ON-BC specificity. We establish proof of concept and provide a translational platform for treatment of CSNB driven by defects in photoreceptor-to-bipolar signaling.

Results

Validation of AAV Capsid Variants. Two AAV capsid variants, $AAV^{K9\#4}$ and $AAV^{K9\#12}$, were selected following a screen for ON-BC targeting in dogs (*SI Appendix*, Figs. S1 and S2) and subsequent testing in a nonhuman primate (NHP) using a long version of a modified mGluR6 (*GRM6*) promoter (*lg*GRM6) (21). The $AAV^{K9\#4}$ and $AAV^{K9\#12}$ capsids were each selected based on their superior capacity for ON-BC–specific expression when injected via subretinal and intravitreal routes, respectively. *In vivo* confocal scanning laser ophthalmoscopy (cSLO) imaging in WT dogs injected with $AAV^{K9\#4}$-*lg*GRM6-*sfGFP* (superfolder green fluorescent protein) subretinally in one eye and $AAV^{K9\#12}$-*lg*GRM6-*sfGFP* intravitreally in the contralateral eye (3×10^{13} vg/mL) showed a strong sfGFP fluorescent signal in the subretinally treated bleb area and in the central to midperipheral retina of the intravitreally injected eye (Fig. 1*A*). Further, IHC confirmed tropism of both vectors to ON-BCs (Fig. 1 *B* and *C*). Quantification of Goα-positive cells showed that intravitreal $AAV^{K9\#12}$ transduced 34 to 86% (central), 0 to 45% (midperiphery), and 0 to 3% (periphery) of ON-BCs (Fig. 1 *C* and *D*). Transduction efficiency with $AAV^{K9\#4}$ in the subretinal bleb area was more homogeneous, ranging from 57% (periphery) to 80% (center) (Fig. 1 *B* and *D*).

To assess the applicability of the selected vectors in both subretinal and intravitreal routes of delivery, reporter constructs $AAV^{K9\#4}$-*lg*GRM6-*sfGFP* and $AAV^{K9\#12}$-*lg*GRM6-*tdTomato* were injected in a cynomolgus macaque. In one eye, both vectors were injected via routes per the canine study, whereas injection routes were switched in the contralateral eye (i.e., $AAV^{K9\#4}$ intravitreally and $AAV^{K9\#12}$ subretinally) (*SI Appendix*, Fig. S3). cSLO autofluorescence imaging performed 6 wk postinjection showed distinct spatial patterns of sfGFP fluorescence between the two eyes. With subretinal injection, both vectors led to transgene expression in ON-BCs throughout the bleb/treated area, with a higher transduction rate with $AAV^{K9\#4}$ (93%) than with $AAV^{K9\#12}$ (80%). Intravitreal injection of either vector led to expression of reporter proteins in ON-BCs in limited areas, including the fovea and punctate areas as detected by cSLO. At the level of the fovea/perifovea, transgene expression in ON-BCs was more potent with $AAV^{K9\#12}$ than with $AAV^{K9\#4}$ when injected intravitreally.

Development of AAV-*LRIT3* Vectors and Assessment of Safety. To test effective targeting of ON-BCs in the canine CSNB model, therapeutic vectors harboring WT c*LRIT3* were constructed. For efficient transgene expression in ON-BCs, two ON-BC–specific promoters were selected—the *lg*GRM6 promoter (2.2 kb) used in prior testing with reporter genes and its abbreviated version *sh*GRM6 (0.7 kb), both developed and validated by Lu et al. (21) for increased and specific transduction of ON-BCs compared with the commonly used 200En (200-bp mGluR6 enhancer) + SV40 (simian virus 40) promoter in mouse and NHP retinas. Of the two, the *lg*GRM6 promoter was reported to have greater transduction efficiency but reduced packaging capacity due to its length. To alleviate this challenge, two versions of the expression cassette were constructed. Cassette A utilized the *lg*GRM6 promoter upstream of WT c*LRIT3* complementary DNA (cDNA) and a polyA signal (Fig. 2*A*). Cassette B instead utilized the *sh*GRM6 promoter, and a woodchuck hepatitis virus posttranscriptional regulatory element (WPRE) was added in between the c*LRIT3* and polyA signal (Fig. 2*B*). WPRE has been suggested to increase AAV-mediated transgene expression through enhancing either RNA processing or nuclear export (22–25). Each expression cassette was then packaged into $AAV^{K9\#4}$ and $AAV^{K9\#12}$ capsids, generating four AAV vector variants.

In a pilot study for evaluating initial tolerability, each vector was injected in control dogs via the intended route (i.e., $AAV^{K9\#4}$ subretinally and $AAV^{K9\#12}$ intravitreally) at doses considered relatively high for intraocular injections (up to 1×10^{13} vg/mL) (*SI Appendix*, Table S2). The two $AAV^{K9\#12}$ vectors were administered intravitreally as intended. The two $AAV^{K9\#4}$ vectors were administered via the intended subretinal route, although some intravitreal vector leakage occurred during subretinal injections and was recorded. Importantly, no acute or delayed adverse

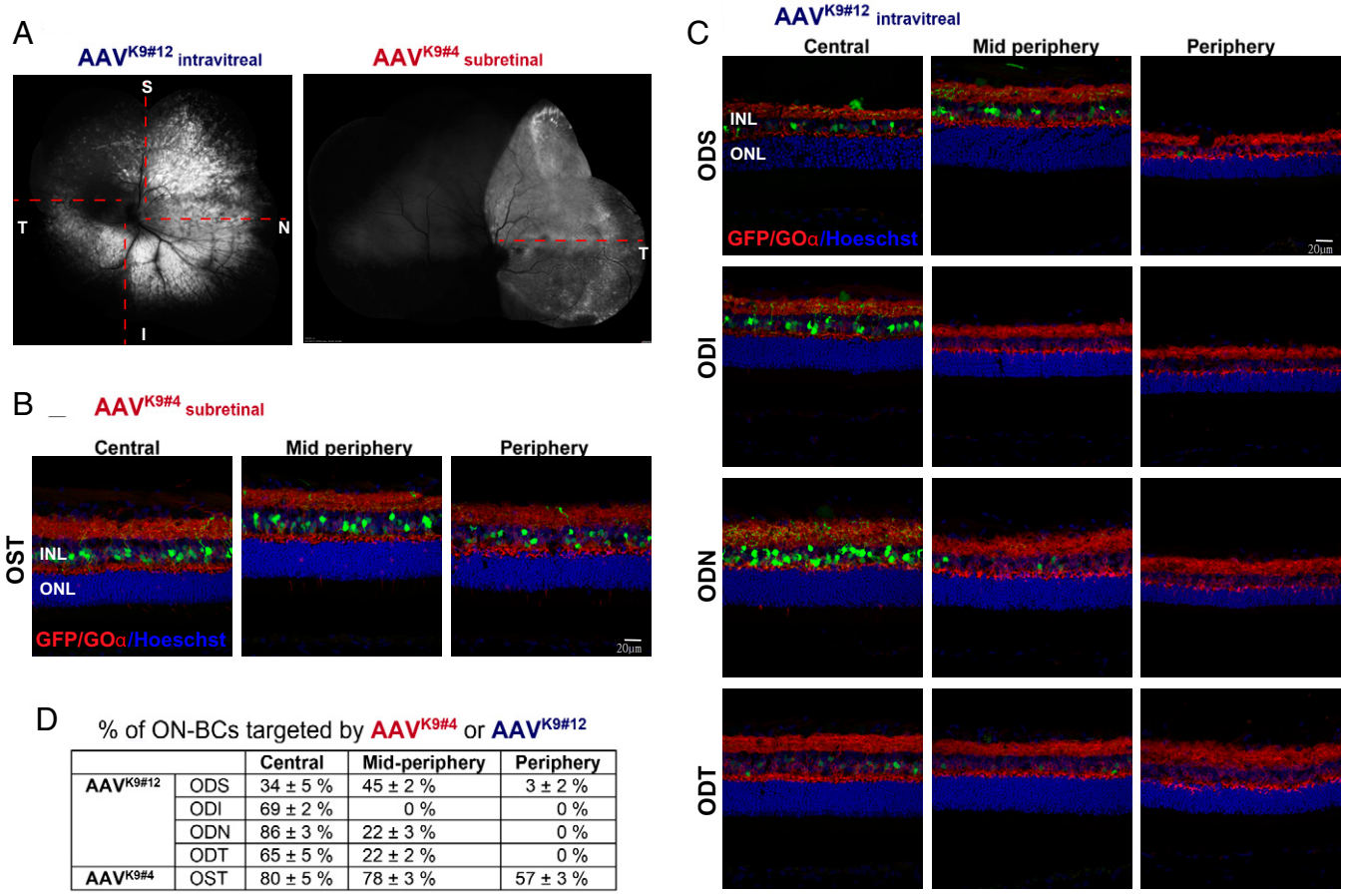

		Central	Mid-periphery	Periphery
AAV$^{K9\#12}$	ODS	34 ± 5 %	45 ± 2 %	3 ± 2 %
	ODI	69 ± 2 %	0 %	0 %
	ODN	86 ± 3 %	22 ± 3 %	0 %
	ODT	65 ± 5 %	22 ± 2 %	0 %
AAV$^{K9\#4}$	OST	80 ± 5 %	78 ± 3 %	57 ± 3 %

Fig. 1. Targeting of canine ON-BCs with top-performing AAV capsid variants. (*A*) cSLO images (blue autofluorescence mode) showing sfGFP fluorescence 6.6 wk after intravitreal injection of AAV$^{K9\#12}$-*lg*GRM6-*sfGFP* (0.38 mL at 2 × 10^{13} vg/mL) in the right eye and subretinal injection of AAV$^{K9\#4}$-*lg*GRM6-*sfGFP* (0.15 mL at 3 × 10^{13} vg/mL) in the left eye. The dashed red lines show approximate locations of the retinal cryosections used for IHC and shown in *B* and *C*. (*B* and *C*) Retinal cryosections showing native sfGFP fluorescence and Goα immunolabeling. (*D*) Percentage of ON-BCs (Goα positive) that coexpress the sfGFP transgene in various retinal locations (n = 3 technical replicates per eye). I, inferior; INL, inner nuclear layer; N, nasal; OD, right eye; ONL, outer nuclear layer; OS, left eye; S, superior; T, temporal.

effects were observed for up to 10 wk postinjection in any of the control eyes as determined by a complete ophthalmic examination, including indirect ophthalmoscopy and fundus imaging.

Restoration of ERG b-wave following Subretinal AAV$^{K9\#4}$-*sh*GRM6-c*LRIT3*-WPRE. To test therapeutic efficacy, the four AAV-*LRIT3* vectors were each injected via the intended route in CSNB dogs (Table 1). Of the eight eyes/four dogs injected in cohort 1, two eyes that received subretinal injection of AAV$^{K9\#4}$-*sh*GRM6-c*LRIT3*-WPRE (Fig. 3*A*) showed significant scotopic b-wave recovery of up to 30% of WT as early as 8 wk postinjection, which remained stable at 51 wk postinjection (Fig. 3*B* and *SI Appendix*, Fig. S5*A*). Of these two eyes, a more dramatic ERG recovery was observed in the eye that received both subretinal delivery (150 μL) and inadvertent intravitreal leakage (200 μL; left eye, CHACUG) compared with the eye with subretinal delivery only (left eye, K10) (Fig. 3*B*). None of the other vectors resulted in measurable ERG recovery and were hence deemed "nontherapeutic." Subsequent studies were focused on the "therapeutic" vector (AAV$^{K9\#4}$-*sh*GRM6-c*LRIT3*-WPRE).

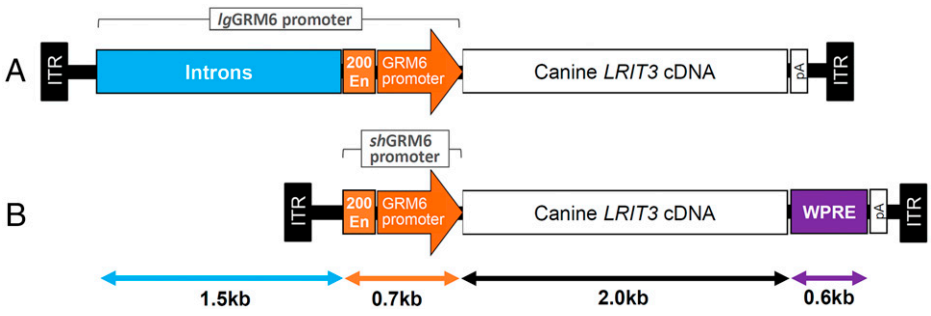

Fig. 2. AAV expression cassette variants including GRM6 promoter variants and c*LRIT3* transgene. Schematic diagram of (*A*) AAV-*lg*GRM6-c*LRIT3* and (*B*) AAV-*sh*GRM6-c*LRIT3*-WPRE cassettes consisting of enhancers (introns, 200En) and the GRM6 promoter driving c*LRIT3*. Due to limitations in packaging capacity, vector A lacks WPRE, while vector B lacks the introns and a large part of the enhancers. ITR, inverted terminal repeat; pA, polyA.

Table 1. Injection details of efficacy testing in *LRIT3*-CSNB dogs

Dog identification	*LRIT3*	Sex	Age at injection (y)	Eye	Route	Vector	Dose level			ERG rescue	End point (months PI)
							vg/mL	mL	vg per eye		
Cohort 1											
K6	−/−	M	1.6	OD	IVT	AAV$^{K9\#12}$-***lg***GRM6-c*LRIT3*	1×10^{13}	0.20	2.0×10^{12}	No	13
				OS	SR	AAV$^{K9\#4}$-***lg***GRM6-c*LRIT3*	1×10^{13}	0.15	1.5×10^{12}	No	
CHACRY	−/−	M	2.8	OD	IVT	AAV$^{K9\#12}$-***lg***GRM6-c*LRIT3*	1×10^{13}	0.20	2.0×10^{12}	No	13
				OS	IVT	AAV$^{K9\#12}$-***sh***GRM6-c*LRIT3*-**WPRE**	1×10^{13}	0.20	2.0×10^{12}	No	
CHACUG	−/−	M	2.8	OD	SR	AAV$^{K9\#4}$-***lg***GRM6-c*LRIT3*	1×10^{13}	0.15	1.5×10^{12}	No	13+
				OS	SR*	AAV$^{K9\#4}$-***sh***GRM6-c*LRIT3*-**WPRE**	1×10^{13}	0.15 + 0.20 (IVT)	3.5×10^{12}	Yes	
K10	−/−	M	1.3	OD	IVT	AAV$^{K9\#12}$-***sh***GRM6-c*LRIT3*-**WPRE**	1×10^{13}	0.20	2.0×10^{12}	No	13
				OS	SR	AAV$^{K9\#4}$-***sh***GRM6-c*LRIT3*-**WPRE**	1×10^{13}	0.15	1.5×10^{12}	Yes	
Cohort 2											
K11	−/−	M	1.6	OD	SR	AAV$^{K9\#4}$-***sh***GRM6-c*LRIT3*-**WPRE**	1×10^{13}	0.10	1.0×10^{12}	Yes	15
				OS	SR*	AAV$^{K9\#4}$-***sh***GRM6-c*LRIT3*-**WPRE**	1×10^{13}	0.13 + 0.12 (IVT)	2.5×10^{12}	Yes	
K16	−/−	M	1.3	OD	SR*	AAV$^{K9\#4}$-***sh***GRM6-c*LRIT3*-**WPRE**	1×10^{13}	0.10 + 0.15 (IVT)	2.5×10^{12}	Yes	15+
				OS	SR	AAV$^{K9\#4}$-***sh***GRM6-c*LRIT3*-**WPRE**	1×10^{13}	0.10	1.0×10^{12}	Yes	

Unique defining features of each vector are indicated in bold. IVT, intravitreal injection; M, male; OD, right eye; OS, left eye; PI, postinjection; SR, subretinal injection.
*SR injection with notable IVT leakage.

Based on the greater b-wave recovery observed with concomitant intravitreal leakage, the effect of combined subretinal and intravitreal injections of the therapeutic vector was tested in cohort 2. Two dogs received a combined subretinal and intravitreal injection in one eye and subretinal only in the other (Table 1). This time, there was no significant difference between ERG b-wave recovery between the different routes of injection (subretinal + intravitreal vs. subretinal only), with both resulting in comparable rod ERG b-wave rescue in one of the two dogs (*SI Appendix*, Fig. S5 *B*, K11). Across both cohorts, the eyes subretinally injected with the therapeutic vector had a rod-derived ERG b-wave amplitude that was significantly increased compared with eyes treated with other vectors/routes at each time point. The effect was evident as soon as 7 wk postinjection ($P < 0.005$) and thereafter, remained robust until at least 64 wk postinjection ($P < 0.001$) (Fig. 3 *C*, *1*). There was no consistent effect on cone-derived ERG associated with specific vectors and injection routes (Fig. 3 *C*, *2* and *SI Appendix*, Fig. S6).

Improved Night Vision in the Eyes Treated with Subretinal AAV$^{K9\#4}$-*sh*GRM6-c*LRIT3*-WPRE. To evaluate the effect of gene therapy on scotopic visual function, injected animals were tested for their ability to navigate in an obstacle avoidance course under scotopic and photopic conditions. Each eye was tested individually using an occluder to block vision in the eye not being tested. While decreased visual acuity has been reported in patients with Schubert–Bornschein CSNB (6, 26), the predominant phenotype is loss of night vision. Moreover, as we have not observed evident day vision defects in *LRIT3*-CSNB dogs (19), testing was done under the three dimmest scotopic conditions (0.003, 0.009, and 0.03 lx) to assess night vision, while a photopic condition (65 lx) was used as the control. The CSNB control eye (Fig. 4 and *SI Appendix*, Fig. S7, white bars) had increased transit times and more collisions at the dimmest light intensity (0.003 lx) as expected from the disease (19). The phenotype was less prevalent as the light intensity was increased under scotopic conditions (0.009 and 0.03 lx) and normalized at the photopic condition (65 lx). All six CSNB eyes subretinally injected with the therapeutic vector (AAV$^{K9\#4}$-*sh*GRM6-c*LRIT3*-WPRE) recovered night vision, resulting in significantly faster transit times and fewer collisions at the dimmest light intensity (Fig. 4, Movies S1 and S2, and *SI Appendix*, Fig. S7, solid orange bars) consistent with the observed ERG recovery. Interestingly, eyes subretinally injected with the vector containing the longer promoter (AAV$^{K9\#4}$-*lg*GRM6-c*LRIT3*), which did not result in ERG recovery, showed a modest trend of visual rescue at 0.003 lx (*SI Appendix*, Fig. S7, solid blue bars). All other vectors injected intravitreally (*SI Appendix*, Fig. S7, hatched orange bars) showed no improvement in night vision (Movies S1 and S2). Strikingly, the recovered night vision was sustained until at least 43 wk postinjection (Movie S2), indicating stability of the therapeutic effect. All CSNB eyes, regardless of the injections, demonstrated normal day vision at 65 lx (Movies S1 and S2), as expected.

Restoration of LRIT3 in the OPL of Canine CSNB Retina. To localize LRIT3 transgene expression in canine retinas injected with AAV vectors, IHC was performed using antibodies against LRIT3 as well as a variety of pre- and postsynaptic markers. Dogs with the best therapeutic response were retained to assess potential lifetime stability of functional rescue. However, one dog with only modest scotopic b-wave recovery in the eye that was subretinally injected with the therapeutic vector (Fig. 3 *A* and *B*, K10, left eye) was euthanized for immunohistochemical analysis of the retina along with controls. LRIT3 signal was detected in the OPL in WT canine retina (Fig. 5 *A*, *D*, and *G*). In this

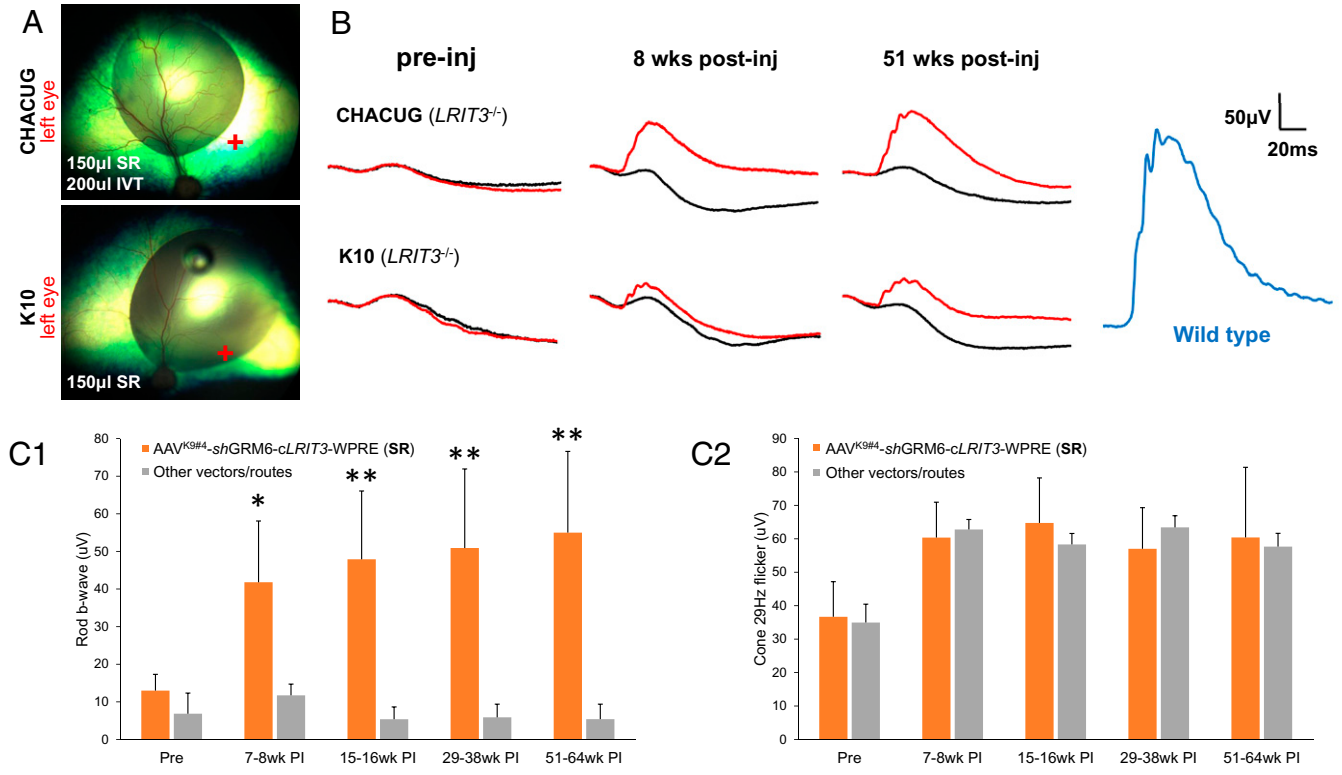

Fig. 3. Subretinal AAV-*LRIT3* injection and ERG recovery in CSNB canine eyes. (*A*) Subretinal blebs in the left eye of dogs CHACUG and K10 that received subretinal injection of the therapeutic vector AAV$^{K9\#4}$-*sh*GRM6-c*LRIT3*-WPRE. Note the injection variables between the two eyes such as bleb location as well as intravitreal vector leakage (200 µL) that occurred in CHACUG. +, canine fovea-like region. (*B*) Rod-derived ERG b-wave recovery in treated eyes shown in *A*. Preinjection ERG traces demonstrate the typical CSNB phenotype with diminished b-wave in both eyes. The eyes receiving subretinal injection of the therapeutic vector show significant b-wave recovery as early as 7 wk postinjection, with stability up to 64 wk postinjection. (*C*) Rod-derived ERG b-wave (*C*, *1*) and cone-derived 29-Hz flicker response (*C*, *2*) pre- and postinjection over time up to 64 wk. The eyes subretinally injected with the therapeutic vector (n = 6; orange bars) had significant and stable rod-mediated ERG b-wave recovery compared with all other vectors/routes (n = 6; gray bars) at each postinjection time points. PI, postinjection; SR, subretinal injection. *P < 0.005; **P < 0.001.

group, LRIT3 labeling appeared to be associated with the synapses between the photoreceptor (postsynaptic density protein 95 [PSD95]) and second-order neurons (Goα) (Fig. 5*A*), present in synapses between rods (C-terminal binding protein 2 [CtBP2]) and rod ON-BCs (protein kinase C alpha [PKCα]) (Fig. 5*D*), and present in synapses between cones (human cone arrestin [hCAR]) (Fig. 5*G*) and all ON-BCs (Goα) (Fig. 5*A*). This signal was greatly reduced in retinas of CSNB dogs (20). In the eye

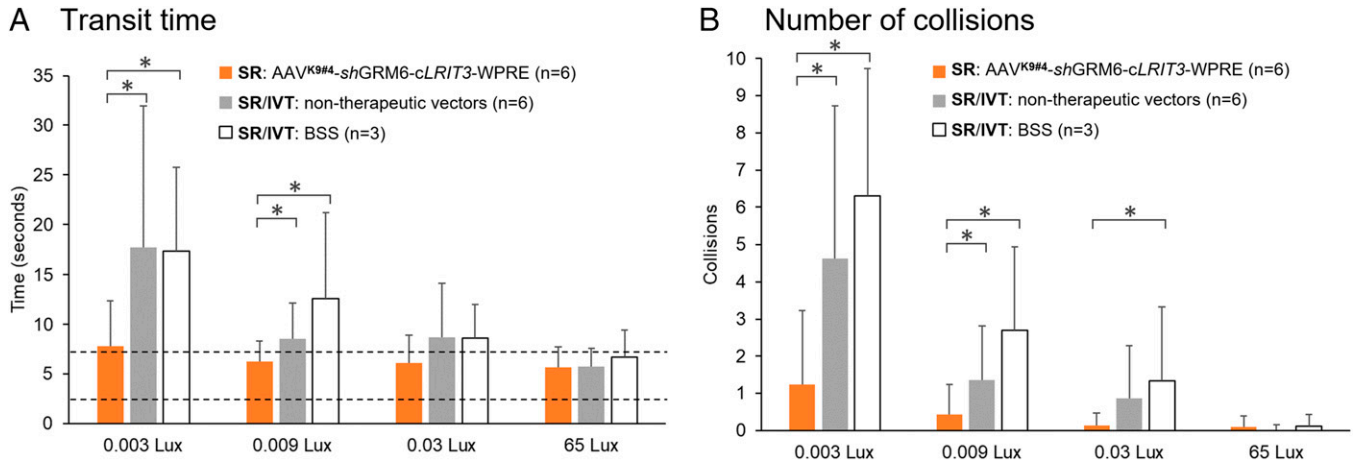

Fig. 4. Improved night vision in CSNB canine eyes treated with subretinal AAV$^{K9\#4}$-*sh*GRM6-c*LRIT3*-WPRE. Visually guided navigation was tested per eye in an obstacle course in six *LRIT3*-CSNB dogs (12 eyes) injected with one of the AAV vector variants in each eye. (*A*) The transit time was significantly reduced following subretinal injection of the therapeutic vector (AAV$^{K9\#4}$-*sh*GRM6-c*LRIT3*-WPRE; six eyes) compared with the eyes injected with all other vectors/routes (six eyes) or BSS-injected control CSNB eyes at the two dimmest scotopic conditions, 0.003 and 0.009 lx. The transition times at 65 lx (photopic) were minimally affected by the CSNB phenotype and as such, comparable across different therapeutic and control groups. The dotted lines define the 95% CIs for transit time in four WT control dogs. *P < 0.0001. (*B*) The number of collisions was significantly reduced at 0.003 and 0.009 lx in eyes subretinally injected with the therapeutic vector (six eyes) compared with CSNB eyes injected with all other vectors/routes (six eyes) or BSS. No collisions are observed in WT dogs. While the bars represent the combined data of three available time points 18 to 50 wk after the injection, there were no significant changes in vision testing outcomes over time. IVT, intravitreal; SR, subretinal. *P < 0.0001.

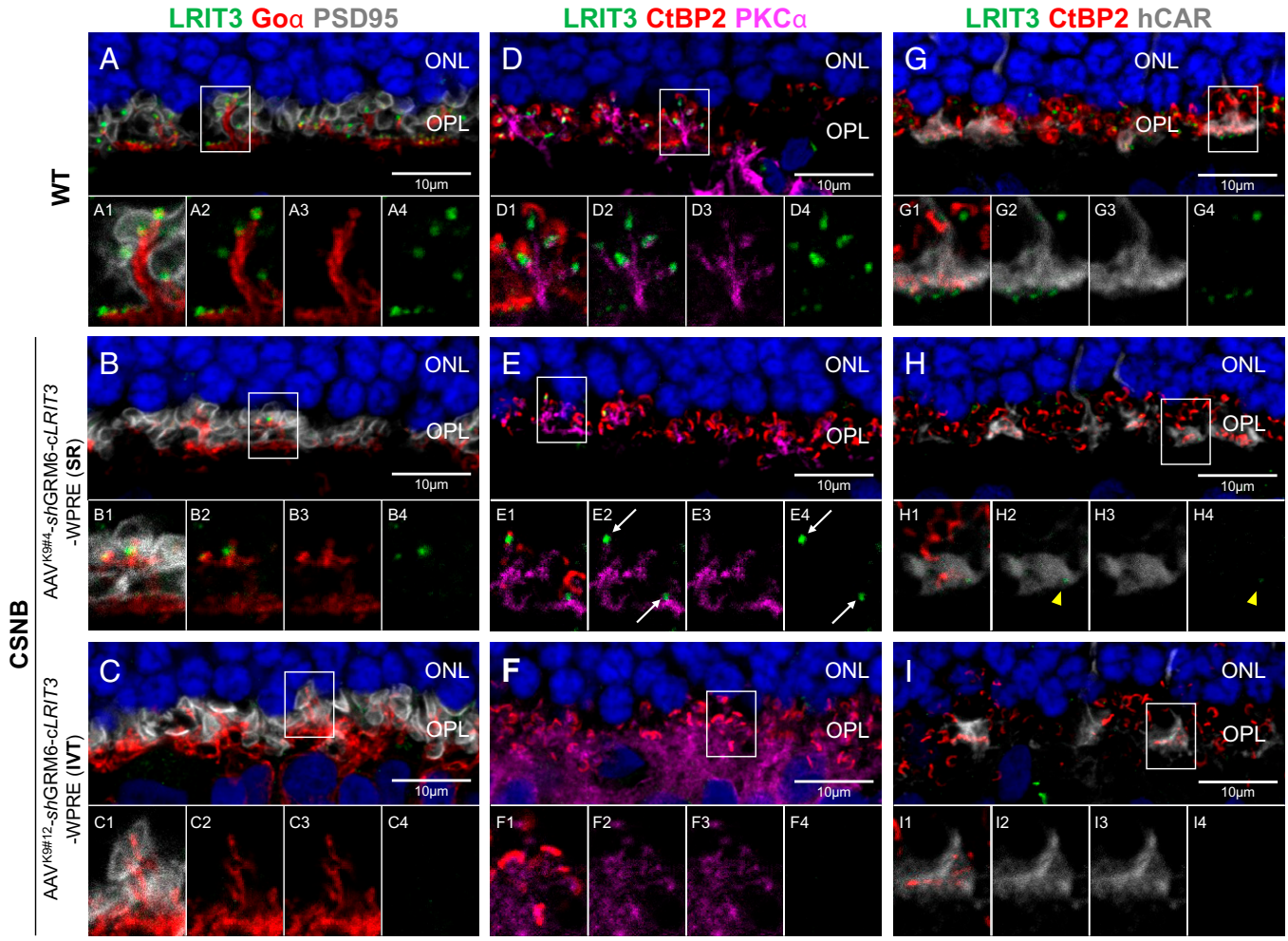

Fig. 5. Restoration of LRIT3 in OPL of canine CSNB retina treated with subretinal AAV-*LRIT3*. WT and CSNB canine retinas were immunolabeled for LRIT3 together for a variety of pre- and postsynaptic markers. WT canine retina (*A*, *D*, and *G*) exhibits punctate LRIT3 signals in OPL adjacent to rod (*D1*) and cone (*G1*) terminals. LRIT3 signal is restored, albeit to a limited amount, in the bleb area of canine CSNB retina treated with subretinal AAV-*LRIT3* and showing ERG recovery (*B*, *E*, and *H*). Restored LRIT3 signal is present adjacent to the synaptic terminals of both rods (*E*, arrows) and cones (*H*, arrowheads). Canine CSNB retina treated with intravitreal AAV-*LRIT3* without ERG recovery (*C*, *F*, and *I*) lacked the LRIT3 signals in OPL. *A–I*, *Lower* are magnified images of the area outlined in *Upper*. Displayed are IHC signals of LRIT3 and both markers merged (*A1–I1*), one of the markers merged with (*A2–I2*) or without (*A3–I3*) LRIT3, and LRIT3 only (*A4–I4*). IVT, intravitreal; ONL, outer nuclear layer; SR, subretinal.

treated with subretinal injection of the therapeutic vector, there was limited but distinct LRIT3 signal restored in the OPL within the bleb area, adjacent to both rod (Fig. 5*E*) and cone terminals (Fig. 5*H*). No signal was present outside of the bleb area in the same eye. The canine CSNB eye intravitreally injected with one of the nontherapeutic vectors (AAV$^{K9\#12}$-*sh*GRM6-c*LRIT3*-WPRE) (*SI Appendix*, Figs. S4–S6, dog CHACRY, left eye) had no evidence of punctate LRIT3 labeling (Fig. 5 *C*, *F*, and *I*). These findings indicate that subretinal delivery of the therapeutic vector and expression of the transgene restores LRIT3 to the OPL and contributes to the structural functionality of the synapse by positioning itself in the normal location at lower levels compared with WT.

Discussion

In a canine model of *LRIT3*-CSNB, we demonstrate safety and efficacy of an AAV gene therapy approach using AAV capsid variants and improved mGluR6 promoters, each designed to specifically target ON-BCs. Phenotypic reversal was assessed by ERG and vision-guided behavior revealing functional restoration with 100% efficacy in all six eyes injected subretinally with the therapeutic vector AAV$^{K9\#4}$-*sh*GRM6-c*LRIT3*-WPRE, providing excellent proof of concept.

We based our approach on previously successful AAV gene therapies delivered to outer retinal cells (i.e., retinal pigmented epithelium, rod, cone) in canine inherited retinal disease models (27–33). Two AAV capsid variants that originated from a prior directed evolution screen conducted in WT dogs (34) were found to specifically target ON-BCs via intravitreal (AAV$^{K9\#12}$) or subretinal (AAV$^{K9\#4}$) injections in WT dogs. Subsequently, these same variants were shown to effectively transduce ON-BCs in NHP. These variants constitute tools for gene therapy to treat patients with various forms of cCSNB and for delivery of optogenetic channels to these midretinal cell populations in patients with advanced photoreceptor degeneration.

Combining each capsid with two different mGluR6 promoters, we tested four unique vector constructs and identified a single "therapeutic vector" (AAV$^{K9\#4}$-*sh*GRM6-c*LRIT3*-WPRE) candidate. This therapeutic vector, when injected subretinally, consistently led to significant and stable functional rescue in all six treated eyes. However, there were some noticeable variations in the degree of phenotypic rescue as quantified by recovery of the scotopic b-wave amplitude, which measured up to 30% of

that of WT. It is important to note that only a limited area of the retina covered by the bleb was treated, leaving a greater area of the retina untreated, likely contributing to incomplete b-wave recovery. Further, there is a limited and varied transduction rate of targeted cells within the treated area, all possible factors affecting the ERG output. Possible injection-related factors affecting phenotypic rescue between eyes include inadvertent intravitreal leakage of vector during the subretinal injection procedure and/or location of the subretinal bleb relative to the area centralis.

The hypothesis that combined subretinal and intravitreal delivery of therapeutic vector provides superior efficacy to subretinal delivery alone remains to be confirmed. While the therapeutic vector was originally optimized for subretinal injection, its ability to transduce ON-BC solely via the intravitreal route remains to be tested. Nevertheless, in our experience, some degree of intravitreal deposition of vectors is expected when performing subretinal injections, and varying degrees of vector exposure interaction with vitreous humor are inevitable. It is, therefore, critical that vectors intended for subretinal delivery are assessed both for toxicity risks and for potential transduction benefits resulting from intravitreal leakage.

The current study was conceived prior to the report by Hasan et al. (35), which proposed an alternative presynaptic localization of LRIT3 in the mouse retina. While this localization may be mouse specific, the gene therapy presented herein was designed for specific targeting of ON-BCs to deliver functional *LRIT3* in the *LRIT3*-CSNB canine model. The AAV vectors used were identified following a screen in WT dogs and selected for ON-BC tropism when administered by subretinal or intravitreal routes. Furthermore, the *sh*GRM6 promoter, derived as a modified version of the mGluR6 (*GRM6*) promoter, was developed and verified by Lu et al. (21) for specific and increased ON-BC expression in mouse and NHP retinas. In our study, subretinal injection of the vector–promoter–reporter constructs in NHP clearly demonstrated ON-BC expression. However, prior to moving toward clinical trials with our ON-BC targeting vector, it will be critically important to determine if targeting photoreceptors instead of ON-BCs results in comparable treatment efficacy as in mice (35, 36).

While the cell type– and species-specific expression of LRIT3 in the retina has not yet been resolved, functional rescue from specific targeting of ON-BCs via AAV gene therapy in the *LRIT3*-CSNB dogs is striking and sheds light on both cell type–specific expression and the optimal functional location of LRIT3. Hasan et al. (35) reported ERG recovery in *Lrit3*$^{-/-}$ mice receiving AAV-*Lrit3* targeted to the rod photoreceptors, but this was successful only with early treatment at P5 and had limited effect when treatment was started later at P30 (*SI Appendix*, Table S1). Interestingly, there was rod-specific transgene expression following injection at either time point (35), suggesting that physical augmentation of LRIT3 in rods may not always restore function in mature retina, thus limiting its translational potential. In a recent report by Varin et al. (36), adult *Lrit3*^{nob6} mice were treated intravitreally using AAV2-7m8-*Lrit3*, targeting ON-BCs alone, photoreceptors alone, or both (OPL) by interchanging cell-specific promoters. Restoration of LRIT3 and TRPM1 localization and functional rescue were demonstrated in only a fraction (7 to 25%) of the treated mice (*SI Appendix*, Table S1). While targeting of either or both cells resulted in a few responsive animals, the rate and degree of functional recovery were greater when targeting photoreceptors followed by OPL and then, ON-BCs, again pointing to potential species-specific differences. In our current work, functional recovery was achieved in adult *LRIT3*-CSNB dogs treated at ages ranging from 1.3 to 2.8 y, demonstrating therapeutic efficacy in mature retina with the CSNB phenotype in 100% (six of six) of eyes injected subretinally with the therapeutic vector targeting ON-BCs. Future work will evaluate if efficacy is improved if *LRIT3*-CSNB animals are treated at a younger age and if augmentation therapy is effective in animals older than 3 y of age.

The therapeutic vector was the only one of four vectors tested resulting in scotopic ERG b-wave functional rescue. However, of the three nontherapeutic vectors, subretinal injection of AAV$^{K9\#4}$-*lg*GRM6-c*LRIT3* resulted in modest improvement of scotopic vision-guided behavior parameters in two dogs compared with controls, despite having no detectable recovery of rod b-wave function. This indicates that the *lg*GRM6-c*LRIT3* expression cassette may be functional, albeit less efficient than the *sh*GRM6-c*LRIT3*-WRPE cassette. In contrast, Lu et al. (21) reported that the *lg*GRM6 promoter was more efficient than *sh*GRM6, suggesting that other factors could affect the expression efficiency in our study, such as improved expression driven by WPRE or interference due to the expression cassette nearing maximum capacity, which was the case for *lg*GRM6-c*LRIT3*.

The mildly improved scotopic function in the eye receiving subretinal AAV$^{K9\#4}$-*lg*GRM6-c*LRIT3* was only detectable by a vision-guided obstacle course navigation and not by ERG, indicating that the former outcome measure is more sensitive for detecting minor functional recovery with potential clinical relevance. This is consistent with the previous assessment of therapeutic outcomes in Leber congenital amaurosis (LCA) patients receiving AAV therapy (37, 38) and reemphasizes the importance of incorporating intuitive and straightforward vision-guided behavior as an outcome assessment of therapy. None of the vectors that utilized the AAV$^{K9\#12}$ capsid designed for intravitreal injection were therapeutically effective. While the initial screening of this AAV capsid variant was done in intact canine eyes, pretreatment of diseased eyes with vitrectomy or enzymatic vitreolysis (39) may improve access of the vector to the retinal layers.

We hereby demonstrate safety and efficacy of an AAV gene therapy designed to target ON-BCs in the *LRIT3*-CSNB canine model. Significant and consistent functional recovery was achieved up to 1.2 y postinjection as assessed by ERG and vision-guided behavior testing. This is patient-relevant data showing rescue of ON-BC function by gene augmentation therapy using a translationally suitable large animal model of *LRIT3*-CSNB. With intact retinal architecture and reliable and validated outcome measures available, the *LRIT3*-CSNB canine model has translational applicability for determination of optimal treatment strategy for CSNB patients. In addition, the model will serve more broadly as a platform to test therapeutic products that target OPL. As the evolving narrative for cell-type expression of native LRIT3 in mature retina is further refined, it will guide our quest to identify and test the most optimal therapeutic targets for the treatment of *LRIT3*-CSNB.

Materials and Methods

Ethics Statement. The research was conducted in strict accordance with the recommendations in the *Guide for the Care and Use of Laboratory Animals* (40) of the NIH and in full compliance with the US Department of Agriculture's Animal Welfare Act, Animal Welfare Regulations, and the ARVO Statement for the Use of Animals in Ophthalmic and Vision Research. The protocols were approved by the Institutional Animal Care and Use Committee (IACUC) of the University of Pennsylvania (IACUC no. 803269) and Charles River Laboratories.

Animals. The *LRIT3*-CSNB model originated from a research colony that was used for disease characterization (19) and mutation identification (20). The dogs in the current study are part of a newly established *LRIT3*-CSNB research line developed at the Retinal Disease Studies Facility (RDSF) of the University of Pennsylvania and were formed by outcrossing dogs from the original colony (19) to WT dogs and to unrelated dogs that had been identified to harbor the *LRIT3* variant through molecular screening. Both control (WT and *LRIT3*-CSNB carrier) and affected dogs, including an *NPHP5*-LCA dog used in AAV vector screening, were bred at the RDSF or by a commercial laboratory animal supplier, and they were maintained and housed at the RDSF under identical conditions of diet, medications, vaccinations, and ambient illumination with cyclic 12-h ON–12-h OFF. CSNB-affected dogs were identified based on genotyping of the *LRIT3* genetic variant (20) and the characteristic loss of scotopic ERG b-wave (19). A single adult male cynomolgus macaque housed at Charles River Laboratories was used in this study to validate the ON-BC tropism of top-performing variants identified following a screen in WT dogs.

Promoter and AAV Capsid Screen for Bipolar Cell Targeting. Eight different AAV capsid variants originating from an AAV2-7-mer library that had undergone directed evolution screens in dogs (34) for their ability to target the outer retina after intravitreal injection were selected together with $AAV2_{4YF+TV}$ (used as a control) for this current study (*SI Appendix*, Table S3). Each of these nine capsids was used individually to package a recombinant genome containing the ON-BC–specific promoter Ins4s-In3-200En-mGluR500p (named thereafter *lg*GRM6) (21), driving expression of sfGFP followed by a 3′ barcode unique to that capsid. The vectors were diluted until the titers of all variants were equal, as confirmed by real-time qPCR, and then, combined in equal ratios by adding equivalent volumes of each vector solution to a pool. A similar approach was used to produce a second pool containing the same nine AAV capsids carrying sfGFP cDNA with the unique barcode but under control of the 4xGRM6 (41) ON-BC–specific promoter. A third pool of the same AAVs was also made but with the Ple155 (42) ON-BC–specific promoter. The latter two pools showed lack of ON-BC specificity when injected intravitreally or subretinally with $AAV2_{4YF+TV}$ vector and were not developed further for this study.

sfGFP-Barcoded Library Screening in Canine Retina. Seven weeks following subretinal (one eye) and intravitreal (two eyes) injections in two WT dogs, biopsies of neuroretina taken from eyes enucleated after humane euthanasia were collected from locations in which sfGFP fluorescence was detected by cSLO. RNA was purified from these samples, and deep sequencing was performed to quantify the relative extents to which each capsid was capable of delivering and expressing its transgene in the canine neuroretina from both the vitreous and subretinal spaces. Quantification of AAV capsid performance revealed that $AAV^{K9\#12}$ and $AAV^{K9\#4}$ outperformed other variants when delivered via the intravitreal and subretinal routes, respectively, and thus, they were selected for further validation.

AAV-*LRIT3* Viral Constructs. To identify the most optimal expression cassette for robust and stable therapeutic gene expression, AAV expression cassette variants *lg*GRM6-c*LRIT3* and *sh*GRM6-c*LRIT3*-WRPE were constructed (Fig. 2). In both variants, the therapeutic gene consisted of full-length c*LRIT3* cDNA, with a canonical Kozak sequence incorporated at the translational initiation site. The c*LRIT3* sequence was cloned from WT canine retinal cDNA, verified by Sanger sequencing, and corrected for polymorphic changes in amino acids to match those of the canine reference genome (CamFam3.1) and of the consensus across mammalian species. Improved mGluR6 promoters developed by Lu et al. (21) aimed at targeting ON-BCs were provided by Zhuo-Hua Pan, Wayne State University, Detroit, MI. The c*LRIT3* transgene was placed under the control of either the original full-length promoter [In4s-In3-200En-mGluR500P (21), *lg*GRM6] or the shortened promoter [200En-mGluR500P (21), *sh*GRM6]. For increased transcript expression, a WPRE sequence was added downstream of the transgene with the *sh*GRM6 promoter. This was not possible with the *lg*GRM6 promoter due to packaging capacity limitations. The two construct variants were each packaged into $AAV^{K9\#4}$ and $AAV^{K9\#12}$ capsids selected via directed evolution for subretinal and intravitreal injections, respectively, as described above. AAV vectors were produced by triple-plasmid cotransfection purified and titered as previously described (43).

Vector Administration and Postinjection Treatment. Under general anesthesia, viral vectors were delivered by subretinal or intravitreal injections in control and affected canine eyes (Table 1 and *SI Appendix*, Table S2 show animals, vectors, and injection details in CSNB dogs and control dogs, respectively) as well as in a single NHP. Viral vectors were diluted in sterile balanced salt solution (BSS) and delivered 100 to 200 μL per eye. A transvitreal approach was used without vitrectomy via pars plana by using a custom-modified subretinal injector with a 39-gauge polyimide cannula (Retinaject; Surmodics, Inc.) (44, 45) under direct visualization through a Machemer magnifying lens (OMVI; Ocular Instruments Inc.) using an operating microscope. Subretinal delivery was directed at the superotemporal quadrant aiming to form a large uniform bleb, encompassing ∼20 to 40% of the retina (*SI Appendix*, Fig. S4), which was immediately visualized and documented by fundus photography (RetCam Shuttle; Natus Medical, Inc.). Intravitreal delivery was performed by deposition of viral solution in the posterior vitreous just preretinally at four sites horizontally across the visual streak. Anterior chamber paracentesis was performed immediately postinjection to prevent an increase in intraocular pressure. The postinjection antibiotic and antiinflammatory routine treatment plan has been described previously (28).

Ophthalmic Examination. Ophthalmic examinations included slit-lamp biomicroscopy, tonometry, indirect ophthalmoscopy, and fundus photography. Any abnormalities, including any development of inflammation or lesions, were documented. The ophthalmic examinations were conducted preinjection, 1- and 2-d postinjection, weekly for the following 4 wk, biweekly for an additional 8 wk, and then, every 12 to 16 wk up to 64 wk postinjection.

ERG. Recordings were conducted at preinjection and then, at postinjection time points of 7 to 8, 15 to 16, 29 to 38, and 51 to 64 wk after vector delivery. Pupils were dilated with topical atropine sulfate 1% (Akorn, Inc.), tropicamide 1% (Akorn, Inc.), and phenylephrine 10% (Paragon Biotech). After induction with intravenous propofol (Zoetis), dogs were maintained under general inhalation anesthesia (isoflurane 2 to 3%; Akorn, Inc.). Full-field flash ERG was performed on both eyes using a custom-built Ganzfeld dome fitted with light-emitting diode stimuli from a ColorDome stimulator (Diagnosys LLC). After 20 min of dark adaptation, rod and mixed rod–cone-mediated responses to single 4-ms white flash stimuli of increasing intensities (−3.7 to 0.5 log $cd{\cdot}s{\cdot}m^{-2}$) were recorded. After 5 min of white light adaptation (10.6 $cd{\cdot}m^{-2}$), cone-mediated responses to a series of single white flashes (−2.7 to 0.5 log $cd{\cdot}s{\cdot}m^{-2}$) and to 29.4-Hz flicker stimuli (−2.7 to 0.2 log $cd{\cdot}s{\cdot}m^{-2}$) were recorded. Finally, photopic long-flash ERGs were recorded using 200-ms white stimuli of 400 $cd.m^{-2}$ on a rod-suppressing white background of 10.6 $cd.m^{-2}$ to assess the ON and OFF pathways. Statistical significance was calculated by an unpaired *t* test using GraphPad (GraphPad Software).

Obstacle Course Vision Testing. Vision-guided navigation was tested in an obstacle avoidance course as previously described (46). An abbreviated protocol was used for this study under the three dimmest scotopic conditions (0.003, 0.009, and 0.03 lx) and under ambient photopic condition (65 lx, fluorescent room light). Each eye was tested individually by having an Aestek opaque corneoscleral shield (Oculo-plastik Inc.) placed over the ocular surface of the contralateral eye after topical anesthesia (proparacaine 0.5%). All eyes were tested three times under each light intensity, and the positions of the five panels were randomly changed between each of the three trials per eye per illumination. The contralateral eye was tested with the same set of panel positions. The eye to be tested was randomly selected before the session. Animals were first dark adapted for 20 min to the lowest ambient illumination (0.003 lx) before running through the course. After testing under scotopic conditions, room illumination was increased to the photopic brightness to light adapt the animals for 10 min, and animals were tested under photopic conditions in the same manner. Two digital Sony Handycam DCR-DVD108 cameras (Sony) located above the obstacle course recorded navigation performance of the dogs. The infrared imaging function of the camera enabled recording under the dimmest light conditions. An experienced observer who was masked to experimental design reviewed all videos and measured for each trial the total number of collisions and transit time in seconds between first forward motion at course entrance and the moment the animal completely passed through the exit gate. Vision testing was repeated at least three times on different dates postinjection to ensure intertesting consistency. An

unpaired *t* test was carried out using GraphPad (GraphPad Software) to analyze statistical significance in the number of collisions and transit time under each illumination level between groups with a cutoff of probability (P) < 0.0001.

IHC. Preparation and processing of tissues for retinal morphology and IHC have been detailed previously (20, 28). Antibodies used included GFP (Millipore; catalog no. MAB3580; Abcam; catalog no. ab290), tdTomato (SICGEN; catalog no. AB8181-200), LRIT3 (Sigma-Aldrich; catalog no. HPA013454), presynaptic markers PSD95 (BioLegend; catalog no. 810401), goat anti-human CAR (custom) and CtBP2 (BD Biosciences; catalog no. 612044), and postsynaptic markers PKCα (BD Biosciences; catalog no. 610107) and Goα (Millipore; catalog no. MAB3073). Slides were examined with a Nikon A1R confocal microscope (Nikon Instruments Inc.). Digital images were captured and processed using the NIS Elements (Nikon Instruments Inc.) and ImageJ software (NIH).

Data Availability. All study data are included in the article and/or supporting information.

ACKNOWLEDGMENTS. We thank Dr. Mineo Kondo of Mie University and Mr. Kazuhiko Sakai and Mr. Takehiro Aihara of Kitayama Labes, Japan for providing foundation dogs for the establishment of the canine CSNB research colony. Additional foundation dogs were generous donations from Labcorp Drug Development, formerly Covance. The *lg*GRM6 and *sh*GRM6 promoters were provided by Dr. Zhuo-Hua Pan of Wayne State University. We also thank Ms. Courtney Spector (formerly of the University of Pennsylvania) for technical assistance, Dr. András Komáromy (Michigan State University) for procedural instructions, and Dr. Leslie King (University of Pennsylvania) for critical review of the manuscript. This study was supported, in part, by the Margaret Q. Landenberger Research Foundation (K.M.), National Eye Institute/NIH Grant EY-006855 (to K.M. and G.D.A.), the Foundation Fighting Blindness (W.A.B. and G.D.A.), the Van Sloun Foundation for Canine Genetic Research (G.D.A.), and the Sanford and Susan Greenberg End Blindness Outstanding Achievement Prize (to G.D.A.).

Author affiliations: [a]Division of Experimental Retinal Therapies, Department of Clinical Sciences & Advanced Medicine, School of Veterinary Medicine, University of Pennsylvania, Philadelphia, PA 19104; [b]Department of Molecular and Cell Biology, University of California, Berkeley, CA 94720; [c]Ophthalmology Services, Charles River Laboratories, Mattawan, MI 49071; and [d]Department of Ophthalmology, University of Pittsburgh School of Medicine, Pittsburgh, PA 15213

1. C. Koike *et al.*, TRPM1 is a component of the retinal ON bipolar cell transduction channel in the mGluR6 cascade. *Proc. Natl. Acad. Sci. U.S.A.* **107**, 332–337 (2010).
2. M. Neuillé *et al.*, LRIT3 is essential to localize TRPM1 to the dendritic tips of depolarizing bipolar cells and may play a role in cone synapse formation. *Eur. J. Neurosci.* **42**, 1966–1975 (2015).
3. C. Zeitz, A. G. Robson, I. Audo, Congenital stationary night blindness: An analysis and update of genotype-phenotype correlations and pathogenic mechanisms. *Prog. Retin. Eye Res.* **45**, 58–110 (2015).
4. L. A. Riggs, Electroretinography in cases of night blindness. *Am. J. Ophthalmol.* **38**, 70–78 (1954).
5. G. Schubert, H. Bornschein, Analysis of the human electroretinogram. *Ophthalmologica* **123**, 396–413 (1952).
6. Y. Miyake, K. Yagasaki, M. Horiguchi, Y. Kawase, T. Kanda, Congenital stationary night blindness with negative electroretinogram. A new classification. *Arch. Ophthalmol.* **104**, 1013–1020 (1986).
7. N. T. Bech-Hansen *et al.*, Loss-of-function mutations in a calcium-channel alpha1-subunit gene in Xp11.23 cause incomplete X-linked congenital stationary night blindness. *Nat. Genet.* **19**, 264–267 (1998).
8. C. M. Pusch *et al.*, The complete form of X-linked congenital stationary night blindness is caused by mutations in a gene encoding a leucine-rich repeat protein. *Nat. Genet.* **26**, 324–327 (2000).
9. I. Audo *et al.*, TRPM1 is mutated in patients with autosomal-recessive complete congenital stationary night blindness. *Am. J. Hum. Genet.* **85**, 720–729 (2009).
10. Z. Li *et al.*, Recessive mutations of the gene TRPM1 abrogate ON bipolar cell function and cause complete congenital stationary night blindness in humans. *Am. J. Hum. Genet.* **85**, 711–719 (2009).
11. M. M. van Genderen *et al.*, Mutations in TRPM1 are a common cause of complete congenital stationary night blindness. *Am. J. Hum. Genet.* **85**, 730–736 (2009).
12. T. P. Dryja *et al.*, Night blindness and abnormal cone electroretinogram ON responses in patients with mutations in the GRM6 gene encoding mGluR6. *Proc. Natl. Acad. Sci. U.S.A.* **102**, 4884–4889 (2005).
13. C. Zeitz *et al.*, Mutations in GRM6 cause autosomal recessive congenital stationary night blindness with a distinctive scotopic 15-Hz flicker electroretinogram. *Invest. Ophthalmol. Vis. Sci.* **46**, 4328–4335 (2005).
14. I. Audo *et al.*, Whole-exome sequencing identifies mutations in GPR179 leading to autosomal-recessive complete congenital stationary night blindness. *Am. J. Hum. Genet.* **90**, 321–330 (2012).
15. N. S. Peachey *et al.*, GPR179 is required for depolarizing bipolar cell function and is mutated in autosomal-recessive complete congenital stationary night blindness. *Am. J. Hum. Genet.* **90**, 331–339 (2012).
16. C. Zeitz *et al.*; Congenital Stationary Night Blindness Consortium, Whole-exome sequencing identifies LRIT3 mutations as a cause of autosomal-recessive complete congenital stationary night blindness. *Am. J. Hum. Genet.* **92**, 67–75 (2013).
17. M. Neuillé *et al.*, Lrit3 deficient mouse (nob6): A novel model of complete congenital stationary night blindness (cCSNB). *PLoS One* **9**, e90342 (2014).
18. M. Neuillé *et al.*, LRIT3 differentially affects connectivity and synaptic transmission of cones to ON- and OFF-bipolar cells. *Invest. Ophthalmol. Vis. Sci.* **58**, 1768–1778 (2017).
19. M. Kondo *et al.*, A naturally occurring canine model of autosomal recessive congenital stationary night blindness. *PLoS One* **10**, e0137072 (2015).
20. R. G. Das *et al.*, Genome-wide association study and whole-genome sequencing identify a deletion in LRIT3 associated with canine congenital stationary night blindness. *Sci. Rep.* **9**, 14166 (2019).
21. Q. Lu *et al.*, AAV-mediated transduction and targeting of retinal bipolar cells with improved mGluR6 promoters in rodents and primates. *Gene Ther.* **23**, 680–689 (2016).
22. J. E. Donello, J. E. Loeb, T. J. Hope, Woodchuck hepatitis virus contains a tripartite posttranscriptional regulatory element. *J. Virol.* **72**, 5085–5092 (1998).
23. J. E. Loeb, W. S. Cordier, M. E. Harris, M. D. Weitzman, T. J. Hope, Enhanced expression of transgenes from adeno-associated virus vectors with the woodchuck hepatitis virus posttranscriptional regulatory element: Implications for gene therapy. *Hum. Gene Ther.* **10**, 2295–2305 (1999).
24. J. E. Loeb, M. D. Weitzman, T. J. Hope, Enhancement of green fluorescent protein expression in adeno-associated virus with the woodchuck hepatitis virus post-transcriptional regulatory element. *Methods Mol. Biol.* **183**, 331–340 (2002).
25. J. C. Paterna, T. Moccetti, A. Mura, J. Feldon, H. Büeler, Influence of promoter and WHV post-transcriptional regulatory element on AAV-mediated transgene expression in the rat brain. *Gene Ther.* **7**, 1304–1311 (2000).
26. K. Ruether, E. Apfelstedt-Sylla, E. Zrenner, Clinical findings in patients with congenital stationary night blindness of the Schubert-Bornschein type. *Ger. J. Ophthalmol.* **2**, 429–435 (1993).
27. G. M. Acland *et al.*, Gene therapy restores vision in a canine model of childhood blindness. *Nat. Genet.* **28**, 92–95 (2001).
28. G. D. Aguirre *et al.*, Gene therapy reforms photoreceptor structure and restores vision in NPHP5-associated Leber congenital amaurosis. *Mol. Ther.* **29**, 2456–2468 (2021).
29. W. A. Beltran *et al.*, Gene therapy rescues photoreceptor blindness in dogs and paves the way for treating human X-linked retinitis pigmentosa. *Proc. Natl. Acad. Sci. U.S.A.* **109**, 2132–2137 (2012).
30. A. V. Cideciyan *et al.*, Mutation-independent rhodopsin gene therapy by knockdown and replacement with a single AAV vector. *Proc. Natl. Acad. Sci. U.S.A.* **115**, E8547–E8556 (2018).
31. K. E. Guziewicz *et al.*, *BEST1* gene therapy corrects a diffuse retina-wide microdetachment modulated by light exposure. *Proc. Natl. Acad. Sci. U.S.A.* **115**, E2839–E2848 (2018).
32. A. M. Komáromy *et al.*, Gene therapy rescues cone function in congenital achromatopsia. *Hum. Mol. Genet.* **19**, 2581–2593 (2010).
33. G. J. Ye *et al.*, Safety and efficacy of AAV5 vectors expressing human or canine CNGB3 in CNGB3-mutant dogs. *Hum. Gene Ther. Clin. Dev.* **28**, 197–207 (2017).
34. B. E. Öztürk *et al.*, scAAVengr, a transcriptome-based pipeline for quantitative ranking of engineered AAVs with single-cell resolution. *eLife* **10**, e64175 (2021).
35. N. Hasan *et al.*, Presynaptic expression of LRIT3 transsynaptically organizes the postsynaptic glutamate signaling complex containing TRPM1. *Cell Rep.* **27**, 3107–3116.e3 (2019).
36. J. Varin *et al.*, Substantial restoration of night vision in adult mice with congenital stationary night blindness. *Mol. Ther. Methods Clin. Dev.* **22**, 15–25 (2021).
37. D. C. Chung *et al.*, Novel mobility test to assess functional vision in patients with inherited retinal dystrophies. *Clin. Exp. Ophthalmol.* **46**, 247–259 (2018).
38. S. Russell *et al.*, Efficacy and safety of voretigene neparvovec (AAV2-hRPE65v2) in patients with RPE65-mediated inherited retinal dystrophy: A randomised, controlled, open-label, phase 3 trial. *Lancet* **390**, 849–860 (2017).
39. P. Stalmans *et al.*; MIVI-TRUST Study Group, Enzymatic vitreolysis with ocriplasmin for vitreomacular traction and macular holes. *N. Engl. J. Med.* **367**, 606–615 (2012).
40. National Research Council, *Guide for the Care and Use of Laboratory Animals* (National Academies Press, Washington, DC, ed. 8, 2012).
41. T. Cronin *et al.*, Efficient transduction and optogenetic stimulation of retinal bipolar cells by a synthetic adeno-associated virus capsid and promoter. *EMBO Mol. Med.* **6**, 1175–1190 (2014).
42. C. N. de Leeuw *et al.*, rAAV-compatible minipromoters for restricted expression in the brain and eye. *Mol. Brain* **9**, 52 (2016).
43. J. G. Flannery, M. Visel, Adeno-associated viral vectors for gene therapy of inherited retinal degenerations. *Methods Mol. Biol.* **935**, 351–369 (2013).
44. W. A. Beltran *et al.*, rAAV2/5 gene-targeting to rods:dose-dependent efficiency and complications associated with different promoters. *Gene Ther.* **17**, 1162–1174 (2010).
45. A. M. Komáromy, S. E. Varner, E. de Juan, G. M. Acland, G. D. Aguirre, Application of a new subretinal injection device in the dog. *Cell Transplant.* **15**, 511–519 (2006).
46. M. M. Garcia, G. S. Ying, C. A. Cocores, J. C. Tanaka, A. M. Komáromy, Evaluation of a behavioral method for objective vision testing and identification of achromatopsia in dogs. *Am. J. Vet. Res.* **71**, 97–102 (2010).